JAERI-Research
97-059

# CONSISTENT ANALYSIS OF COLLECTIVE LEVEL STRUCTURE AND NEUTRON INTERACTION DATA FOR $^{12}C$ IN THE FRAMEWORK OF THE SOFT-ROTATOR MODEL

September 1997

Efrem Sh. SUKHOVITSKIĬ*, Yurij V. PORODZINSKIĬ*
Osamu IWAMOTO and Satoshi CHIBA

日本原子力研究所
Japan Atomic Energy Research Institute

本レポートは，日本原子力研究所が不定期に公刊している研究報告書です。
入手の問合わせは，日本原子力研究所研究情報部研究情報課（〒319-11 茨城県那珂郡東海村）あて，お申し越しください。なお，このほかに財団法人原子力弘済会資料センター（〒319-11 茨城県那珂郡東海村日本原子力研究所内）で複写による実費頒布をおこなっております。

This report is issued irregularly.
Inquiries about availability of the reports should be addressed to Research Information Division, Department of Intellectual Resources, Japan Atomic Energy Research Institute, Tokai-mura, Naka-gun, Ibaraki-ken, 319-11, Japan.



編集兼発行　日本原子力研究所
印　　刷　いばらき印刷㈱

# Consistent Analysis of Collective Level Structure and Neutron Interaction Data for $^{12}C$ in the Framework of the Soft-rotator Model

Efrem Sh. SUKHOVITSKIĬ*, Yurij V. PORODZINSKIĬ*
Osamu IWAMOTO and Satoshi CHIBA

Department of Reactor Engineering
Tokai Research Establishment
Japan Atomic Energy Research Institute
Tokai-mura, Naka-gun, Ibaraki-ken

(Received August 1, 1997)

A systematic analysis of nuclear structure and neutron interaction data for $^{12}C$ was carried out in the framework of the soft-rotator model. The model was firstly applied to analyze the low-lying collective level strucure of the $^{12}C$ nucleus, which turned out to be very successful. The intrinsic wave function obtained in such an analysis was then used to construct the coupling potentials in the coupled-channels formalism to calculate the neutron total and scattering cross sections. The quadrupole deformation parameter obtained in the present analysis was 0.164, which was much smaller in the absolute sense than the value used in the symmetric-rotator, vibrator model employed frequently in the past, i.e., $\approx 0.6$. When averaged over the $\beta$-vibration function, however, the present result yields an effective quadrupole strength of about the same scale as the previous studies due to softness of the $^{12}C$ wave function with respect to $\beta_2$ degree of freedom. The soft-rotator model was found to be very successful in reproducing both the structure and neutron scattering data consistently for the first time in this mass region.

Keywords: Collective Band Structure, $^{12}C$, Soft-rotator Model, Coupled Channel Calculation, Neutron Inelastic Scattering Cross Sections

---

*Radiation Physics and Chemistry Problems Institute

# Soft-rotaror modelによる$^{12}$Cの集団励起構造と中性子反応データの解析

日本原子力研究所東海研究所原子炉工学部
Efrem Sh. SUKHOVITSKIĬ*, Yurij V. PORODZINSKIĬ*
岩本　修・千葉　敏

(1997年8月1日受理)

Soft-rotaror modelを用いて$^{12}$Cの核構造及び中性子との相互作用データの解析を行った。はじめに$^{12}$Cの低集団励起レベル構造の解析を行い、これらのレベルを良く再現できることが分かった。この解析によって得られた内部波動関数は中性子全断面積および散乱断面積の計算のために、チャンネル結合法における結合ポテンシャルの計算に使用した。これらの解析から得られた4重極変形パラメータは0.164であり、過去によく使用されてきたsymmetric-rotator, vibrator modelにより得られる約0.6という値と比べ、かなり小さい値となった。しかし$\beta$振動の関数として平均した4重極の実効的強度は過去の研究のものと同じ程度となっている。これは$^{12}$Cの波動関数の$\beta_2$自由度に対する柔軟性によるものである。この質量数領域においてsoft-rotaror modelはバンド構造及び中性子散乱データをよく再現することが分かった。

東海研究所：〒319－11　茨城県那珂郡東海村白方白根2－4
＊ 放射線物理化学問題研究所

Contents



# 目　　次

# 1. Introduction

The $^{12}C$ nucleus has attracted a good deal of attentions from both the fundamental physics and applications points of view. On the fundamental side, the collective nature of $^{12}C$ has been offering a very good tests for nuclear structure and reaction theories. The $^{12}C$ nucleus shows both rotational and vibrational characters in the low-lying level scheme, although such a structure is not as prominent as the case for heavier nuclei.

The excited states of $^{12}C$ have been discussed by wide variety of models in previous works such as the shell-model[1], $\alpha$-cluster model[2] and by the resonating group method[3]. On the other hand, neutron scattering data have been studied mostly by the symmetric-rotator, vibrator model in the past (see for example the work by Meigooni et al.[4] and Olsson et al.[5]). The absolute value of the quadrupole deformation parameter found in the analysis of scattering data was as large as 0.6, which is beyond the values that have been found recently in the physics of "super" deformed nucleus. It is therefore a matter of big interest whether or not the frequently employed model is applicable in such a very deformed region. Anyway, until now, no consistent attempt has been given, to the authors' knowledge, to describe the low-lying collective level structure and neutron scattering data in a unified framework.

From the applications point of view, the neutron scattering from carbon is very important to assess the neutron-induced absorbed dose in tissue because carbon is one of the four main elements of human tissue. Furthermore, the neutron-carbon interaction is crucially important to evaluate correctly respoonces of many kinds of neutron detectors since carbon is very often the major constituent of such devices.

The purpose of this work is to give a consistent description of the collective nuclear structure and neutron scattering properties of $^{12}C$ in the framework of the soft-rotator model. This model was developed as an extention of the Davydov-Chaban model[8] which takes account of the $\beta$-vibration in non-axial soft rotational nuclei. Here, the word "soft" denotes, for example, a possibility of stretching during the rotation. The present version of the soft-rotator model includes the non-axial quadrupoe, octupole and hexadecapole deformations, and the $\beta_2$-, $\beta_3$- and $\gamma$- vibrations[9, 10, 11, 12, 13]. This model has been extensively applied for similar analyses in heavier mass region. However, this theory has never before been employed for the analysis of the mass region as light as carbon.

We have performed an analysis of nuclear level scheme of $^{12}C$ in terms of the soft-rotator model, which determined the intrinsic carbon wave function. Nextly, this wave function was used to construct the coupling potentials in the coupled-channels formalism in an analysis of neutron scattering data in the energy region of 20 to 40 MeV. We have selected this energy region partly because there is a prominent resonance structure below this energy region which makes the concept of the optical model rather ambiguous, and partly because there is not much neutron scattering data which covers a wide angular region above this energy range.

Details of the soft-rotator model analysis is explained in the following sections. Then, some discussions on the results are given, which is followed by the conclusion.

## 2. Analysis of the collective nuclear structure of $^{12}$C

We assume that excited states observed in even-even non-spherical nuclei can be described as a combination of rotation, $\beta$-quadrupole and octupole vibrations, and $\gamma$-quadrupole vibration. Instant nuclear shapes that correspond to such excitations can be presented [14, 15] in a body fixed system as

$$\begin{aligned} R(\theta',\varphi') &= R_0\left\{1+\sum_{\lambda\mu}\beta_{\lambda\mu}Y_{\lambda\mu}\right\} \\ &= R_0\left\{1+\beta_2\left[\cos\gamma Y_{20}(\theta',\varphi')+\frac{1}{\sqrt{2}}\sin\gamma\left(Y_{22}(\theta',\varphi')+Y_{2-2}(\theta',\varphi')\right)\right]\right. \\ &\quad +\beta_3\left[\cos\eta Y_{30}(\theta',\varphi')+\frac{1}{\sqrt{2}}\sin\eta\left(Y_{32}(\theta',\varphi')+Y_{3-2}(\theta',\varphi')\right)\right] \\ &\quad \left.+b_{40}Y_{40}(\theta',\varphi')+\sum_{\mu=2,4}b_{4\mu}\left(Y_{4\mu}(\theta',\varphi')+Y_{4-\mu}(\theta',\varphi')\right)\right\}. \end{aligned} \tag{1}$$

To simplify the calculations, we assume that internal octupole variables satisfy additional conditions

$$b_{3\pm1} = b_{3\pm3} = 0,\ b_{32} = b_{3-2}, \tag{2}$$

which are admissible in case for first excited states[16].

The Hamiltonian $\hat{H}$ of the soft-rotator model consists of the kinetic energy terms for the rotation of the non-axial nuclei with quadrupole, octupole and hexadecapole deformations, the $\beta_2$-, $\gamma$-quadrupole and octupole vibrations, and the vibrational potentials ignoring a coupling between the 3 vibration modes. Considering nuclei that are rigid with respect to ocutupole transverse vibrations, the Hamiltonian can be written in the form[9]

$$\hat{H} = \frac{\hbar^2}{2B_2}\left\{\hat{T}_{\beta_2}+\frac{1}{\beta_2^2}\hat{T}_\gamma\right\}+\frac{\hbar^2}{2}\hat{T}_r+\frac{\hbar^2}{2B_3}\hat{T}_{\beta_3}+\frac{\beta_{20}^4}{\beta_2^2}V(\gamma)+V(\beta_2)+V(\beta_3), \tag{3}$$

where

$$\hat{T}_{\beta_2} = -\frac{1}{\beta_2^4}\frac{\partial}{\partial\beta_2}\left(\beta_2^4\frac{\partial}{\partial\beta_2}\right), \tag{4a}$$

$$\hat{T}_\gamma = -\frac{1}{\sin 3\gamma}\frac{\partial}{\partial\gamma}\left(\sin 3\gamma\frac{\partial}{\partial\gamma}\right), \tag{4b}$$

$$\hat{T}_{\beta_3} = -\frac{1}{\beta_3^3}\frac{\partial}{\partial\beta_3}\left(\beta_3^3\frac{\partial}{\partial\beta_3}\right). \tag{4c}$$

The symbol $\hat{T}_r$ denotes the operator of deformed nuclear rotational energy expressed in terms of the angular momentum operator $\hat{I}_i$ and principal moments of inertia,

$$\hat{T}_r = \sum_{i=1}^{3}\frac{\hat{I}_i^2}{J_i} = \sum_{i=1}^{3}\frac{\hat{I}_i^2}{J_i^{(2)}+J_i^{(3)}+J_i^{(4)}}. \tag{5}$$

Here $J_i^{(\lambda)}$ stands for the principal moments of inertia in the direction of $i$-th axis in the body-fixed system due to quadrupole, octupole and hexadecapole deformations depending on $\lambda$=2, 3 and 4, respectively. The symbol $\hat{I}_i$ denotes the projection of the angular-momentum operator on the $i$-th axis of the body-fixed coordinate, $\beta_{20}$ denotes the quadrupole equilibrium deformation parameter at the ground state

(G.S.), and $B_\lambda$ the mass parameter for multipolarity of $\lambda$. The eigenfunctions $\Psi$ of operator (3) are defined in the space of six dynamical variables: $0 \le \beta_2 < \infty$, $-\infty < \beta_3 < \infty$, $\frac{n\pi}{3} \le \gamma \le \frac{(n+1)\pi}{3}$, $0 \le \theta_1 \le 2\pi$, $0 \le \theta_2 \le \pi$ and $0 \le \theta_3 < 2\pi$, with the volume element $d\tau = \beta_2^4\beta_3^3|\sin 3\gamma| d\beta_2 d\beta_3 d\gamma d\theta_1 \sin\theta_2 d\theta_2 d\theta_3$. Here $\beta_\lambda^2 = \sum \beta_{\lambda\mu}\beta_{\lambda\mu}^*$ is the measure of nucleus deformation with multipolarity $\lambda$.

For nuclei of shape determined by Eq. (1), $J_i^{(\lambda)}$ are given by

$$J_i^{(2)} = 4B_2\beta_2^2 \sin^2[\gamma - (2/3)\pi i] \tag{6a}$$

$$J_1^{(3)} = 4B_3\beta_3^2 \left(\frac{1}{2}\cos^2\eta + \frac{\sqrt{15}}{4}\sin 2\eta + 1\right), \tag{6b}$$

$$J_2^{(3)} = 4B_3\beta_3^2 \left(\frac{1}{2}\cos^2\eta - \frac{\sqrt{15}}{4}\sin 2\eta + 1\right), \tag{6c}$$

$$J_3^{(3)} = 4B_3\beta_3^2 \sin^2\eta, \tag{6d}$$

$$J_1^{(4)} = 4B_4 \left(\frac{5}{2}b_{40}^2 + 4b_{42}^2 + b_{44}^2 + \frac{3}{2}\sqrt{10}b_{40}b_{42} + \sqrt{7}b_{42}b_{44}\right), \tag{6e}$$

$$J_2^{(4)} = 4B_4 \left(\frac{5}{2}b_{40}^2 + 4b_{42}^2 + b_{44}^2 - \frac{3}{2}\sqrt{10}b_{40}b_{42} - \sqrt{7}b_{42}b_{44}\right), \tag{6f}$$

$$J_3^{(4)} = 4B_4 \left(2b_{42}^2 + 8b_{44}^2\right), \tag{6g}$$

with $b_{4\mu}$ that can be presented [17]

$$b_{40} = \beta_4 \left(\sqrt{7/12}\cos\delta_4 + \sqrt{5/12}\sin\delta_4\cos\gamma_4\right), \tag{7a}$$

$$b_{42} = \beta_4\sqrt{1/2}\sin\delta_4\sin\gamma_4, \tag{7b}$$

$$b_{44} = \beta_4\sqrt{1/2}\left(\sqrt{5/12}\cos\delta_4 - \sqrt{7/12}\sin\delta_4\cos\gamma_4\right), \tag{7c}$$

with $\eta$, $\delta_4$ and $\gamma_4$ -parameters determining non-axiality of ocutupole and hexadegcapole deformations.

For the sake of convenience let's rewrite $\hat{T}_r$:

$$\hat{T}_r = \frac{1}{4B_2\beta_2^2}\sum_{i=1}^{3}\frac{\hat{I}_i^2}{j_i^{(2)} + a_{32}j_i^{(3)} + a_{42}j_i^{(4)}}, \tag{8}$$

where $j_i^{(\lambda)} = J_i^{(\lambda)}/4B_\lambda\beta_\lambda^2$, $a_{\lambda 2} = (B_\lambda/B_2)(\beta_\lambda/\beta_2)^2$. To solve the Schrödinger equation we expand Eq. (8) around the minima of the potential energy of quadrupole and octupole vibrations, i.e., $\beta_{20}$, $\gamma_0$ and $\beta_{30}$:

$$\begin{aligned}\hat{T}_r = {} & \frac{1}{4B_2\beta_2^2}\sum_{i=1}^{3}\left\{\left.\frac{\hat{I}_i^2}{j_i^{(2)} + a_{32}j_i^{(3)} + a_{42}j_i^{(4)}}\right|_{\substack{\beta_2=\beta_{20}\\ \gamma=\gamma_0\\ \beta_3=\beta_{30}}}\right. \\ & + \frac{\partial}{\partial\gamma}\left[\frac{\hat{I}_i^2}{j_i^{(2)} + a_{32}j_i^{(3)} + a_{42}j_i^{(4)}}\right]\Bigg|_{\substack{\beta_2=\beta_{20}\\ \gamma=\gamma_0\\ \beta_3=\beta_{30}}}(\gamma - \gamma_0) \\ & + \frac{\partial}{\partial a_{32}}\left[\frac{\hat{I}_i^2}{j_i^{(2)} + a_{32}j_i^{(3)} + a_{42}j_i^{(4)}}\right]\Bigg|_{\substack{\beta_2=\beta_{20}\\ \gamma=\gamma_0\\ \beta_3=\beta_{30}}} 2a_{320}\left[\frac{\beta_3 \mp \beta_{30}}{\pm\beta_{30}} - \frac{\beta_2 - \beta_{20}}{\beta_{20}}\right] + \cdots\end{aligned}$$

$$-\frac{\partial}{\partial a_{42}}\left[\frac{\hat{I}_i^2}{j_i^{(2)}+a_{32}j_i^{(3)}+a_{42}j_i^{(4)}}\right]\Bigg|_{\substack{\beta_2=\beta_{20}\\ \gamma=\gamma_0\\ \beta_3=\beta_{30}}} 2a_{420}\left[\frac{\beta_2-\beta_{20}}{\beta_{20}}\right]+\cdots\Bigg\}, \tag{9}$$

where $a_{\lambda 20}=(B_\lambda/B_2)(\beta_{\lambda 0}/\beta_{20})^2$ and $\pm$ at $\beta_{30}$ denotes that we bear in mind that even-even octupole deformed nuclei must have two minima $\pm\beta_{30}$ of the potential energy that correspond to two symmetric octupole shapes. These nuclei are characterized by the double degeneration of levels, which is washed out as a result of tunneling transition through the barrier separating those nuclear shapes with opposite values of octupole deformation [18, 19].

In the zero-order approximation the operator of nuclear rotation energy is identical to that $\hat{T}_r$ of a nucleus having quadrupole deformation, provided that the principal moments of inertia are redefined reflecting account of octupole and hexadecapole deformation. Let us change variable $\beta_3=\beta_2\epsilon$ and assume that in the new variables, the potential energy of octupole vibrations assumes the form

$$V(\beta_3)+\frac{3\hbar^2}{8B_3\beta_3^2} = \frac{\hbar^2}{2B_3\mu_\epsilon^4\beta_{20}}(\epsilon\mp\epsilon_0)^2\,. \tag{10}$$

Owing to centrifugal forces caused by nuclear rotation, equilibrium octupole deformations are transformed due to the $\beta_3=\beta_2\epsilon$ in direct proportion with the increase of $\beta_2$. It is shown in [20] that, along with the choice of potential in the form of Eq. (10), this enables us to reproduce various patterns of level-energy intervals observed experimentally for positive and negative parity bands of even-even nuclei.

Let us solve the Schrödinger equation in the zero-order approximation for the expansion of the rotational-energy operator $\hat{T}_r$. Assuming that $\Psi=(\beta_2^{-2}\beta_3^{-3/2})/\sqrt{\sin 3\gamma}\,u$, we arrive at

$$-\frac{\hbar^2}{2B_2}\frac{\partial^2 u}{\partial\beta_2^2}-\frac{\hbar^2}{2B_3\beta_2^2}\frac{\partial^2 u}{\partial\epsilon^2}-\frac{\hbar^2}{2B_2\beta_2^2}\frac{\partial^2 u}{\partial\gamma^2}+\frac{\hbar^2}{2B_2\beta_2^2}\frac{1}{4}\sum_{i=1}^{3}\frac{\hat{I}_i^2}{j_i^{(2)}+a_{32}j_i^{(3)}+a_{42}j_i^{(4)}}\Bigg|_{\substack{\beta_2=\beta_{20}\\ \gamma=\gamma_0\\ \beta_3=\beta_{30}}} u$$
$$+\left[V(\beta_2)+\frac{\hbar^2}{2B_3\mu_\epsilon^4\beta_2^2}(\epsilon\mp\epsilon_0)^2+\frac{\beta_0^4}{\beta_2^2}V(\gamma)-\frac{\hbar^2}{2B_2\beta_2^2}\frac{9}{4}\frac{1+\sin^2 3\gamma}{\sin^2 3\gamma}\right]u = Eu. \tag{11}$$

The quadrupole and octupole variables in (11) are now separated, and the function $u$ can be factorized. Thus we have

$$u = \psi^{\pm}(\beta_2,\gamma,\Theta)\varphi^{\pm}_{n_{\beta_3}}(\epsilon), \tag{12}$$

where

$$\varphi^{\pm}_{n_{\beta_3}}(\epsilon) = \frac{c_{n_{\beta_3}}}{\sqrt{2}}\left[\chi_{n_{\beta_3}}(\tau_\epsilon^+)\pm\chi_{n_{\beta_3}}(\tau_\epsilon^-)\right], \tag{13}$$

$$\tau_\epsilon^{\pm} = \epsilon\mp\epsilon_0\,. \tag{14}$$

Here, $\chi_{n_{\beta_3}}(\tau_\epsilon^{\pm})$ are oscillator functions that satisfy the equation

$$\left[-\frac{\hbar^2}{2B_3}\frac{\partial^2}{\partial\epsilon^2}+\frac{\hbar^2}{2B_3\mu_\epsilon^4}(\epsilon\mp\epsilon_0)^2\right]\chi_{n_{\beta_3}}(\tau_\epsilon^{\pm}) = \hbar\omega_\epsilon(n+1/2)\chi_{n_{\beta_3}}(\tau_\epsilon^{\pm}), \tag{15}$$

where the frequency is given by $\omega_\epsilon=\hbar/(B_3\mu_\epsilon^2)$, $n_{\beta_3}=0,1,2,\cdots$ and $c_{n_{\beta_3}}$ is the normalization constant. The superscript $\pm$ on the eigenfunctions specifies their symmetry under the transformation $\epsilon_0\to-\epsilon_0$.

Nuclear states of positive parity are described by symmetric combinations of the oscillator functions, while states of negative parity are represented by antisymmetric combinations.

The function $\psi^{\pm}(\beta_2,\gamma,\Theta)$ satisfies the equation

$$\frac{\hbar^2\beta^2}{2B_2}\frac{\partial^2\psi^{\pm}}{\partial\beta_2^2}+\frac{\hbar^2}{2B_2}\frac{\partial^2\psi^{\pm}}{\partial\gamma^2}-\frac{\hbar^2}{2B_2}\frac{1}{4}\sum_{i=1}^{3}\frac{\hat{I}_i^2}{j_i^{(2)}+a_{32}j_i^{(3)}+a_{42}j_i^{(4)}}\Bigg|_{\substack{\beta_2=\beta_{20}\\ \gamma=\gamma_0\\ \beta_3=\beta_{30}}}\psi^{\pm}$$
$$-\left[\beta_2^2V(\beta_2)+\beta_0^4V_0(\gamma)-\frac{\hbar^2}{2B_2}\frac{9}{4}\frac{1+\sin^2 3\gamma}{\sin^2 3\gamma}+E^{\pm}_{n_{\beta_3}}-E^{\pm}\beta_2^2\right]\psi^{\pm}\;=\;0, \tag{16}$$

where $E^{\pm}_{n_{\beta_3}}=\hbar\omega_{\epsilon}(n_{\beta_3}+1/2)\mp\delta_n$ is the energy of octupole longitudinal surface vibrations, and $2\delta_n$ is the energy splitting of a doubly degenerate level due to the tunneling effect.

The only difference between equation (16) and the analogous equation (considered in detail in [9]) for vibrational and rotational state of positive parity in non-axial deformed even-even nuclei is due to the necessity of taking into account the dependence of the eigenfunctions of the rotation operator $\hat{T}_r$ on the parity of the states under consideration. If $K$ is even (as in our case), these functions have the form

$$\Phi^{\pm}_{IM\tau}(\Theta)\;=\;\sum_{K\geq 0}|IMK,\pm\rangle\,A^{\tau}_{IK}, \tag{17}$$

where

$$|IMK,\pm\rangle\;=\;((2I+1)/(16\pi^2(1+\delta_{K0})))^{1/2}\left[D^I_{MK}(\Theta)\pm(-1)^I D^I_{M-K}(\Theta)\right], \tag{18}$$

the symbol $D^I_{M\pm K}(\Theta)$ being the rotation function. In even-even nuclei, rotational bands formed by positive parity levels are described by the wave functions $|IMK,+\rangle$ of a rigid rotator, which transform according to the irreducible representation $A$ of the $D_2$ group. Bands formed by negative-parity levels with even $K$ are described by the functions $|IMK,-\rangle$ that realize the irreducible representation $B_1$ of the same group [20].

Using the results from [9], we can obtain the eigenvalues of the nuclear Hamiltonian predicting the energies of rotational-vibrational states (with allowance for the quadrupole and octupole deformability of an even-even nucleus in the zero-order approximation of $\hat{T}_r$ expansion) in the form

$$\begin{aligned}E^{\pm}_{I\tau n_\gamma n_{\beta_3} n_{\beta_2}}\;=\;&\hbar\omega_0\left\{\left(\nu_{I\tau n_\gamma n_{\beta_3} n_{\beta_2}}+1/2\right)\times\left(4-3/P^{\pm}_{I\tau n_\gamma n_{\beta_3}}\right)^{1/2}\right.\\&+\frac{1}{2}\frac{\mu^2_{\beta_{20}}}{P^{\pm 2}_{I\tau n_\gamma n_{\beta_3}}}\left[\frac{2}{\mu^2_{\gamma_0}}(\nu_{n_\gamma}-\nu_{0_\gamma})+\varepsilon^{\pm}_{I\tau}+\epsilon^{\pm}_{n_{\beta_3}}-\epsilon^{+}_{0_{\beta_3}}\right]\\&\left.+\frac{1}{2}\frac{\mu^6_{\beta_{20}}}{P^{\pm 6}_{I\tau n_\gamma n_{\beta_3}}}\left[\frac{2}{\mu^2_{\gamma_0}}(\nu_{n_\gamma}-\nu_{0_\gamma})+\varepsilon^{\pm}_{I\tau}+\epsilon^{\pm}_{n_{\beta_3}}-\epsilon^{+}_{0_{\beta_3}}\right]^2\right\},\end{aligned} \tag{19}$$

where $\epsilon^{\pm}_{n_{\beta_3}}=\frac{2B_2}{\hbar^2}E^{\pm}_{n_{\beta_3}}$, and $P^{\pm}_{I\tau n_\gamma n_{\beta_3}}$ is a root of the equation

$$\left(P^{\pm}_{I\tau n_\gamma n_{\beta_3}}-1\right)P^{\pm 3}_{I\tau n_\gamma n_{\beta_3}}=\mu^{\pm 4}_{\beta_{20}}\left[\frac{2}{\mu^2_{\gamma_0}}(\nu_{n_\gamma}-\nu_{0_\gamma})+\varepsilon^{\pm}_{I\tau}+\epsilon^{\pm}_{n_{\beta_3}}-\epsilon^{+}_{0_{\beta_3}}\right], \tag{20}$$

where $\hbar\omega_0$, $\mu_{\beta_{20}}$, $\mu_{\gamma_0}$ and $\gamma_0$ are the model parameters to be adjusted to reproduce experimentally-known band structures. The $\hbar\omega_0$ parameter denotes an overall scale factor of the level energies, $\mu_{\beta_{20}}$, $\mu_{\gamma_0}$ and $\mu_{\epsilon}$ are related with the elasticity constants of $\beta_2-$, $\gamma-$ and octupole vibrations, respectively,

and $\gamma_0$ is the equilibrium point of the $\gamma-$vibration. Other quantities in the above equation are to be determined in the following way.

The quantity $\varepsilon^{\pm}_{I_\tau}$ is the eigenvalues of the asymmetric-rotator Hamiltonian[21, 22] with principal moments of inertia redefined by equation (9), which is written by

$$\hat{T}_r \Phi^{\pm}_{IM\tau} \;=\; \varepsilon^{\pm}_{I_\tau} \Phi^{\pm}_{IM\tau}. \tag{21}$$

The quantity $\nu_{n_\gamma}$ is determined by a system of the following two equations corresponding to the boundary conditions for $\gamma$-vibrations, and $n_\gamma$ is the number of the solution as $\nu_{n_\gamma}$ is growing.

$$\begin{cases} v_{\nu_{n_\gamma}} \left[ -\dfrac{\sqrt{2}}{\mu_{\gamma_0}} \left( \dfrac{\pi}{3} n - \gamma_0 \right) \right] \;=\; 0 \\ v_{\nu_{n_\gamma}} \left[ -\dfrac{\sqrt{2}}{\mu_{\gamma_0}} \left( \dfrac{\pi}{3} (n+1) - \gamma_0 \right) \right] \;=\; 0 \end{cases}, \tag{22}$$

where $v_{\nu_{n_\gamma}}(y)$ denotes a solution of an oscillator equation

$$\left[ \frac{d^2}{dy^2} + \nu_{n_\gamma} + \frac{1}{2} - \frac{y^2}{4} \right] v_{\nu_{n_\gamma}}(y) \;=\; 0 \tag{23}$$

being a linear combination of two standard non-linear solutions

$$v_{\nu_{n_\gamma}}(y) \;=\; c_{n_\gamma} \left[ D_{\nu_{n_\gamma}}(y) + a_{n_\gamma} V_{\nu_{n_\gamma}}(y) \right], \tag{24}$$

with $D_{\nu_{n_\gamma}}$ -well known Weber function (see [23]). $\nu^{\pm}_{I\tau n_\gamma n_{\beta_3} n_{\beta_2}}$ is determined be boundary conditions (22), but in this case, one of the boundaries is at infinity, and this reduces the possible solution of equation (23)

$$v_\nu(y) \;=\; c_\nu D_\nu(y), \tag{25}$$

so that $\nu^{\pm}_{I\tau n_\gamma n_{\beta_3} n_{\beta_2}}$ is determined by equation

$$D_{\nu^{\pm}_{I\tau n_\gamma n_{\beta_3} n_{\beta_2}}} \left[ -\frac{\sqrt{2} P^{\pm}_{I\tau n_\gamma n_{\beta_3}}}{\mu_{\beta_{20}}} \left( 4 - \frac{3}{P^{\pm}_{I\tau n_\gamma n_{\beta_3}}} \right) \right] \;=\; 0. \tag{26}$$

At last we can write the nuclear wave function

$$\begin{aligned} \Psi^{\pm}_{I\tau n_\gamma n_{\beta_3} n_{\beta_2}} \;=\; & C^{\pm}_{I\tau n_\gamma n_{\beta_3} n_{\beta_2}} \frac{C_{n_{\beta_3}}}{\sqrt{2}} \frac{\beta_2^{-2} \beta_3^{-3/2}}{\sqrt{\sin 3\gamma}} \sum_{K \geq 0} |IMK, \pm\rangle \, A^{\tau}_{IK} \\ & \times D_{\nu^{\pm}_{I\tau n_\gamma n_{\beta_3} n_{\beta_2}}} \left[ \frac{\sqrt{2}}{\beta_{20} \mu^{\pm}_{I\tau n_\gamma n_{\beta_3} n_{\beta_2}}} \left( \beta_2 - \beta^{\pm}_{2_{I\tau n_\gamma n_{\beta_3}}} \right) \right] \\ & \times v_{n_\gamma} \left[ \frac{\sqrt{2}}{\mu_{\gamma_0}} (\gamma - \gamma_0) \right] \left[ \chi_{n_{\beta_3}}(\tau^+_\epsilon) \pm \chi_{n_{\beta_3}}(\tau^-_\epsilon) \right], \end{aligned} \tag{27}$$

with

$$\beta^{\pm}_{2_{I\tau n_\gamma n_{\beta_3}}} \;=\; \beta_{20} P^{\pm}_{I\tau n_\gamma n_{\beta_3}}, \tag{28}$$

which denotes the equilibrium deformation of the stretched rotating nucleus for state $I_{\tau n_\gamma n_{\beta_3}}$ and

$$\frac{1}{\mu^{\pm 4}_{\beta_{2_{I\tau n_\gamma n_{\beta_3}}}}} \;=\; \frac{1}{\mu^4_{\beta_{20}}} + \frac{3 \left[ \frac{2}{\mu^2_{\gamma_0}} \left( \nu_{n_\gamma} - \nu_{0_\gamma} \right) + \varepsilon^{\pm}_{I\tau} + \epsilon^{\pm}_{n_{\beta_3}} - \epsilon^{\pm}_{0_{\beta_3}} \right]}{P^{\pm}_{I\tau n_\gamma n_{\beta_3}}}, \tag{29}$$

with $\mu_{\beta_2 I\tau n_\gamma n_{\beta_3}}$ being the nucleus softness for this state. The correction $\Delta E^{\pm}_{I\tau n_\gamma n_{\beta_3} n_{\beta_2}}$ to the energy of rotational-vibrational states due to linear terms of expansion (9) can be easily calculated by perturbation theory. If we consider $n_{\beta_3} = 0$ ( as states with $n_{\beta_3} \geq 1$ lie above the experimentally resolved) this correction is given by

$$\Delta E^{\pm}_{I\tau n_\gamma n_{\beta_3}(=0) n_{\beta_2}} = \hbar\omega_0 \frac{\mu^2_{\beta_2}}{\beta^2_{20}} \left\{ \frac{B_3}{B_2} \epsilon_0^2 \left\langle \Phi^{\pm}_{IM\tau}(\theta) \right| \sum_{i=1}^{3} \frac{\partial}{\partial a_{32}} \left[ \frac{\hat{I}_i^2}{j_i^{(2)} + a_{32} j_i^{(3)} + a_{42} j_i^{(4)}} \right] \Bigg|_{\substack{\beta_2=\beta_{20} \\ \gamma=\gamma_0 \\ \beta_3=\beta_{30}}} \left| \Phi^{\pm}_{IM\tau}(\theta) \right\rangle \right.$$

$$\times \left\{ \left[ \frac{e^{-\epsilon_0^2/\mu_\epsilon^2}}{1 \pm e^{-\epsilon_0^2/\mu_\epsilon^2}} \left( \frac{\mu_\epsilon}{\epsilon_0\sqrt{\pi}} \pm \frac{\mu_\epsilon}{\epsilon_0\sqrt{\pi}} \mp \right) - \frac{\mathrm{erfc}(\epsilon_0/\mu_\epsilon)}{1 \pm e^{-\epsilon_0^2/\mu_\epsilon^2}} \right] J^{\pm}_{\substack{I\tau n_\gamma n_{\beta_3} n_{\beta_2} \\ I\tau n_\gamma n_{\beta_3} n_{\beta_2}}}(1/y^2) - J^{\pm}_{\substack{I\tau n_\gamma n_{\beta_3} n_{\beta_2} \\ I\tau n_\gamma n_{\beta_3} n_{\beta_2}}}(1/y^2) \right\}$$

$$\left. - \frac{B_4}{B_2} \beta_4^2 \left\langle \Phi^{\pm}_{IM\tau}(\theta) \right| \sum_{i=1}^{3} \frac{\partial}{\partial a_{42}} \left[ \frac{\hat{I}_i^2}{j_i^{(2)} + a_{32} j_i^{(3)} + a_{42} j_i^{(4)}} \right] \Bigg|_{\substack{\beta_2=\beta_{20} \\ \gamma=\gamma_0 \\ \beta_3=\beta_{30}}} \left| \Phi^{\pm}_{IM\tau}(\theta) \right\rangle \times J^{\pm}_{\substack{I\tau n_\gamma n_{\beta_3} n_{\beta_2} \\ I\tau n_\gamma n_{\beta_3} n_{\beta_2}}} \left[ (y-1)/y^2 \right] \right\}, \quad (30)$$

where

$$J^{\pm}_{\substack{I\tau n_\gamma n_{\beta_3} n_{\beta_2} \\ I'\tau' n'_\gamma n'_{\beta_3} n'_{\beta_2}}} [f(y)] = \int_0^\infty f(y) D_{\nu^{\pm}_{I\tau n_\gamma n_{\beta_3} n_{\beta_2}}} \left[ -\frac{\sqrt{2}}{\mu^{\pm}_{I\tau n_\gamma n_{\beta_3}}} \left( y - P^{\pm}_{I\tau n_\gamma n_{\beta_3}} \right) \right]$$

$$\times D_{\nu^{\pm}_{I'\tau' n'_\gamma n'_{\beta_3} n'_{\beta_2}}} \left[ -\frac{\sqrt{2}}{\mu^{\pm}_{I'\tau' n'_\gamma n'_{\beta_3}}} \left( y - P^{\pm}_{I'\tau' n'_\gamma n'_{\beta_3}} \right) \right] dy$$

$$\times \left\{ \int_0^\infty D^2_{\nu^{\pm}_{I\tau n_\gamma n_{\beta_3} n_{\beta_2}}} \left[ -\frac{\sqrt{2}}{\mu^{\pm}_{I\tau n_\gamma n_{\beta_3}}} \left( y - P^{\pm}_{I\tau n_\gamma n_{\beta_3}} \right) \right] dy \right\}^{-1/2}$$

$$\times \left\{ \int_0^\infty D^2_{\nu^{\pm}_{I'\tau' n'_\gamma n'_{\beta_3} n'_{\beta_2}}} \left[ -\frac{\sqrt{2}}{\mu^{\pm}_{I'\tau' n'_\gamma n'_{\beta_3}}} \left( y' - P^{\pm}_{I'\tau' n'_\gamma n'_{\beta_3}} \right) \right] dy' \right\}^{-1/2}. \quad (31)$$

The formulae explained above were applied for a description of the low-lying collective levels of $^{12}$C to get the nuclear Hamiltonian parameters. The experimental level scheme was taken from [26] and is shown in Fig. 1. Rotational bands in the case of $^{12}$C are not very prominent. Nevertheless we could fix two lower levels of ground state rotational band, $0^+$ (0.0 MeV) and $2^+$ (4.44 MeV), and $3^+$ (20.56 MeV) to be the level of $K \approx 2$ band. This allowed us to obtain the values for $\hbar\omega_0$, $\mu_{\beta_{20}}$, $\gamma_0$ which showed that $2^+$, $K \approx 2$ can be assigned to the experimentally measured level with energy 17.6 MeV, the spin of which is not measured. The calculated energy is 17.55 MeV. The experimentally measured $0^+$ (7.65 MeV) level in our scheme appears to be a band head $K = 0$, $n_{\beta_2} = 1$, with predicted energy of 7.72 MeV. The $4^+$ ground state rotational band level is suggested to be at 13.7 MeV, while the experimental energy is 14.08 MeV. A level with spin $2^+$, $K = 0$ and $n_{\beta_2} = 1$ is predicted by our model with energy 11.94 MeV; we think it can be attributed to one of the experimentally measured levels with energies 16.11 and 15.4 MeV, having no spin assignment, as we see no other assignment possibility. One can see that our model permits the description of all the experimentally measured levels of positive parity up to 20 MeV, except those $1^+$, which are not considered (are not of collective nature). We also included $3^-$ (9.64 MeV) in our consideration. The calculated energy is adjusted by varying the parity energy splitting parameter $\delta_{n_{\beta_3}}$. Comparison of calculated and experimental level scheme is presented in Fig. 1. The resulting nuclear Hamiltonian parameters are shown in Table 1.

# 3. Analysis of neutron interaction data

The soft-rotator wave functions determined in the analysis of low-lying level structure as described in the previous section can be utilized as a base for building a coupling scheme for a coupled-channels calculation to describe the nucleon-nucleus interaction for $^{12}$C. As usualy, non-spherical optical potential is taken in a standard form

$$V(r) = -V_R f_R(r) - i\left[4W_D a_D \frac{d}{dr} f_D(r) + W_V f_V(r)\right] + \left(\frac{\hbar}{\mu_\pi c}\right)^2 V_{SO} \frac{1}{r}\frac{d}{dr} f_{so}(r)\hat{\sigma}\hat{L}, \tag{32}$$

with the form factors

$$f_i \;=\; \left[1 + \exp\left(r - R_i\right)/a_i\right]^{-1},\; i = R, V, D, so, \tag{33}$$

whose radii are given by the expression (1). The symbols $i = R, V, D$ and $so$ denote the real volume, imaginary volume, imaginary surface and real spin-orbit potential, respectively. Each of the potential is expanded in a Taylor series considering $\beta_L$ to be a small parameter following the recipes of Tamura[24] for vibrational nuclei, and taking account of the nuclear shape determined by Eq. (1). More spesifically, writing Eq. (1) as $R = R_0 + \delta R$ where $\delta R \equiv R_0 \sum \beta_{\lambda\mu} Y_{\lambda\mu}$, the potential can be expanded in a straight-forward manner as

$$V(R) \;=\; V(R_0) \;+\; \sum_{t=1}^{max} \left.\frac{\partial^t V}{\partial R^t}\right|_{R=R_0} \frac{\delta R^t}{t!} \tag{34}$$

The coupling potential $V_{couple}$ is the matrix element of the second term of this expansion between 2 different soft-rotator model states, and is written in the form

$$V_{couple} \;=\; \sum_{t=1}^{max} \sum_{n=0}^{t} \beta_L^{t-n} \beta_{L'}^{n} v^{(t)}(r) \sum_{\lambda\mu} Q_{\lambda\mu}^{*LL'(t)} Y_{\lambda\mu}(\theta', \varphi'). \tag{35}$$

Here, $v^{(t)}(r)$ are the optical potential derivatives, and the $Q_{\lambda\mu}^{*LL'(t)}$-operator reflects the non-axiality of the nucleaus and the transformation to the space fixed system. We have ignored a term like $\beta_2\beta_3\beta_4$ because usually such a cross term is not significant. The $max$ in the expanstion was taken to be 4. The difference between the calculated coupling potential (and thus the coupling strength) in our model and the rigid rotator approach can be understood as following. Powers of $\beta_L$ and functions of $\gamma$ in $Q_{\lambda\mu}^{*LL'(t)}$ are averaged over wave functions of appropriate initial $|i\rangle$ and final $|f\rangle$ states to obtain the coupling. Usually $\langle i|\beta_L^t|f\rangle/\beta_L^t$ is grater than unity and the enhancement is growing for softer nuclei. As $\langle i|\beta_L^t|f\rangle$ is not equal to $\langle i|\beta_L|f\rangle^t$ and more $\langle i|\beta_L^t|f\rangle$ values differ for different $i$ and $f$, models using $\beta_L$ -constant or effective in coupling schemes calculations do not take into account redistributions of coupling strength for different channels predicted by our model, and describe the dynamic of interaction with the simplification described.

We have included in our coupled-channels (CC) analysis the data at 28.2 MeV from JAERI[25], and other recent neutron scattering data above 20 MeV from Ohio [4], Uppsala [5] and Michigan State Universities [6]. More detailed information about the data involved in the analysis can be found in Table 2.

One can see that we did not include available data with neutron interaction energies below 20 MeV. For such energies, energy loss even for the first $2^+$ (4.44 MeV) excited level decreases the neutron energy

in the outgoing scattering channels to the region with prominent resonance structure in the total cross section and can influence the results of the analysis. We assumed that the interaction of neutrons with $^{12}$C proceeds only via direct mechanism for the chosen energy region. Five levels ($0^+$, $2^+$, $0_2^+$, $3^-$, $2_2^+$) coupling scheme was used in CC calculations, as preliminary numerical results showed that the inclusion of additional levels influences the results by less than experimental errors of the data involved. The coupling scheme appearing and used in our calculation is shown on Fig. 2. We must emphasize that various bands are coupled not only with the ground state band, but also with each other. The significant feature of this scheme is the natural existence of coupling between the levels of different bands without additional assumptions. Such a feature is absent in most of the previous analyses[4, 5].

The optical potential parameters were searched for by minimizing the quantity $\chi^2$, defined by

$$\chi^2 = \frac{1}{N+M}\left[\sum_{i=1}^{N}\frac{1}{K_i}\sum_{j=1}^{K_i}\left(\frac{d\sigma_{ij}/d\omega_{calc}-d\sigma_{ij}/d\omega_{exp}}{\Delta\sigma_{ij}/d\omega_{exp}}\right)^2+\sum_{i=1}^{M}\left(\frac{d\sigma_{tot_{cal_i}}-d\sigma_{tot_{eval_i}}}{\Delta\sigma_{tot_{eval_i}}}\right)^2\right], \quad (36)$$

where $N$ number of experimental scattering data sets, $K_i$ number of angular points in each data set, $M$ number of energies, for which experimental total cross section data[27] is involved. The evaluated total cross section was fitted to the experimental value to improve the optical parameter search. The optical potential parameters allowing the best fit of experimental data are presented in Table 3.

Within the optical parameter search, the parameters of the nuclear Hamiltonian were fixed except for $\mu_{\gamma_0}$ which was adjusted to fit the scattering data, since it was impossible to determine this parameter by analyzing the level scheme, as no levels with $n_\gamma \geq 1$ are observed in $^{12}$C.

One can see that total cross-section of $^{12}$C in the energy region 15-55 MeV (Fig. 3) and experimental scattering data (Fig. 4-7) are described reasonably well by our model. We think that angular distributions of neutrons scattered by $0_2^+$ (7.65 MeV) and $3^-$ (9.64 MeV) levels are much better described than by Meigooni et al.[4] This proves that our nuclear Hamiltonian wave functions for these states are more reliable than the simpler model employed frequently.

# 4. Analysis of B(E2) data

The $\gamma$-transition probability $B(E\lambda)$ of soft rotator model can also be calculated. For instance $B(E2)$ calculated in homogeneously charged deformed ellipsoid approximation accounting linear terms of inner $b_{2\mu}$ dynamic variables (higher terms can be taken into consideration, see [21]) is

$$\begin{aligned}B(E2; I\tau n_\gamma n_{\beta_3} n_{\beta_2} \to I'\tau' n'_\gamma n'_{\beta_3} n'_{\beta_2}) = \frac{5Q_0^2}{16\pi}\Bigg\{\sum_{K,K'\geq 0}\frac{A^{\tau}_{IK}A^{\tau'}_{I'K'}}{[(1+\delta_{0K})(1+\delta_{0K'})]^{1/2}} \\ \times\Big[\langle n_\gamma|\cos\gamma|n'_\gamma\rangle\Big[(I'2K'0|IK)+(-1)^{I'}(I'2-K0|IK)\delta_{K0}\Big]\delta_{KK'} \\ +\sqrt{1/2}\langle n_\gamma|\sin\gamma|n'_\gamma\rangle\left[(I'2K'2|IK)\delta_{K,K'+2}+(I'2K'-2|IK)\delta_{K,K'-2}\right. \\ \left.+(-1)^{I'}(I'2-K'2|IK)\delta_{K,2-K'}\Big]\Big]\Bigg\}^2\left[J^{\,I\tau n_\gamma n_{\beta_3} n_{\beta_2}}_{I'\tau' n'_\gamma n'_{\beta_3} n'_{\beta_2}}[y]\right]^2. \quad (37)\end{aligned}$$

One can see that comparing with the rigid model our $B(E2)$ is enhanced by the factor $J^2$ the square of the already discussed integral over $\beta_2$ variable guiding the enhancement of coupling strength. As in case

in the outgoing scattering channels to the region with prominent resonance structure in the total cross section and can influence the results of the analysis. We assumed that the interaction of neutrons with $^{12}$C proceeds only via direct mechanism for the chosen energy region. Five levels ($0^+$, $2^+$, $0_2^+$, $3^-$, $2_2^+$) coupling scheme was used in CC calculations, as preliminary numerical results showed that the inclusion of additional levels influences the results by less than experimental errors of the data involved. The coupling scheme appearing and used in our calculation is shown on Fig. 2. We must emphasize that various bands are coupled not only with the ground state band, but also with each other. The significant feature of this scheme is the natural existence of coupling between the levels of different bands without additional assumptions. Such a feature is absent in most of the previous analyses[4, 5].

The optical potential parameters were searched for by minimizing the quantity $\chi^2$, defined by

$$\chi^2 = \frac{1}{N+M}\left[\sum_{i=1}^{N}\frac{1}{K_i}\sum_{j=1}^{K_i}\left(\frac{d\sigma_{ij}/d\omega_{calc}-d\sigma_{ij}/d\omega_{exp}}{\Delta\sigma_{ij}/d\omega_{exp}}\right)^2+\sum_{i=1}^{M}\left(\frac{d\sigma_{tot_{cal_i}}-d\sigma_{tot_{eval_i}}}{\Delta\sigma_{tot_{eval_i}}}\right)^2\right], \quad (36)$$

where $N$ number of experimental scattering data sets, $K_i$ number of angular points in each data set, $M$ number of energies, for which experimental total cross section data[27] is involved. The evaluated total cross section was fitted to the experimental value to improve the optical parameter search. The optical potential parameters allowing the best fit of experimental data are presented in Table 3.

Within the optical parameter search, the parameters of the nuclear Hamiltonian were fixed except for $\mu_{\gamma_0}$ which was adjusted to fit the scattering data, since it was impossible to determine this parameter by analyzing the level scheme, as no levels with $n_\gamma \geq 1$ are observed in $^{12}$C.

One can see that total cross-section of $^{12}$C in the energy region 15-55 MeV (Fig. 3) and experimental scattering data (Fig. 4-7) are described reasonably well by our model. We think that angular distributions of neutrons scattered by $0_2^+$ (7.65 MeV) and $3^-$ (9.64 MeV) levels are much better described than by Meigooni et al.[4] This proves that our nuclear Hamiltonian wave functions for these states are more reliable than the simpler model employed frequently.

# 4. Analysis of B(E2) data

The $\gamma$-transition probability $B(E\lambda)$ of soft rotator model can also be calculated. For instance $B(E2)$ calculated in homogeneously charged deformed ellipsoid approximation accounting linear terms of inner $b_{2\mu}$ dynamic variables (higher terms can be taken into consideration, see [21]) is

$$\begin{aligned}B(E2;I\tau n_\gamma n_{\beta_3} n_{\beta_2}\to I'\tau' n'_\gamma n'_{\beta_3} n'_{\beta_2}) = \frac{5Q_0^2}{16\pi}\Bigg\{\sum_{K,K'\geq 0}\frac{A^\tau_{IK}A^{\tau'}_{I'K'}}{[(1+\delta_{0K})(1+\delta_{0K'})]^{1/2}}\\ \times\Big[\langle n_\gamma|\cos\gamma|n'_\gamma\rangle\Big[(I'2K'0|IK)+(-1)^{I'}(I'2-K0|IK)\delta_{K0}\Big]\delta_{KK'}\\ +\sqrt{1/2}\langle n_\gamma|\sin\gamma|n'_\gamma\rangle\left[(I'2K'2|IK)\delta_{K,K'+2}+(I'2K'-2|IK)\delta_{K,K'-2}\right.\\ \left.+(-1)^{I'}(I'2-K'2|IK)\delta_{K,2-K'}\right]\Big]\Bigg\}^2\left[J^{I\tau n_\gamma n_{\beta_3} n_{\beta_2}}_{I'\tau' n'_\gamma n'_{\beta_3} n'_{\beta_2}}[y]\right]^2. \quad (37)\end{aligned}$$

One can see that comparing with the rigid model our $B(E2)$ is enhanced by the factor $J^2$ the square of the already discussed integral over $\beta_2$ variable guiding the enhancement of coupling strength. As in case

of coupling probabilities of $\gamma$-transition from and to different levels are enhanced differently coupling with the rigid rotator model.

We compared the $B(E2)$ transition probability with the experimental data. Our model predicts 0.00418 $e^2b^2$ while the experimental value is $0.0041e^2b^2$[28]. Considering the fact that no parameter was adjusted to calculate this quantity, the agreement can be marked to be fantstic.

# 5. Discussion

According to the microscopic 3$\alpha$ cluster model[2, 3], the $0_1^+$, $2_1^+$ (4.44MeV) and $4_1^+$ (14.08MeV) are classified to form a ground state rotational band with a compact 3$\alpha$-cluster configurations around an equilateral triangle. Although the present model does not take account of such $\alpha$-cluster structure, the classification into a rotational band is also achieved in our model. The energy of the $4_1^+$ state is slightly less than the one expected from the rigid rotor model if the moment of inertia is calculated according to the energy of the $2_1^+$ state. The soft-rotator model accounts for such a stretching effect, as shown in Fig. 1. Firthermore, the $\alpha$ cluster model suggest a strong K-mixing in the $2_2^+$ and $3^+$ states, which is in good agreement with the present result because of the large $\gamma_0$ value.

In previous works[4, 5], the symmetric rotational model was employed to analyze the neutron scattering data, and $^{12}$C was assumed to have a large oblate deformation ($\beta_2 \approx$ -0.6), which is in good accord with the microscopic $\alpha$ cluster model[3]. On the other hand, there is no symmetry axis in the present tri-axial model. Indeed, the non-axiality parameter has a large value ($\gamma_0 = 0.3210$) compared with the case for actinide, so the axial symmetry is broken to a large extent in $^{12}$C. Therefore, the present model gives a different picture of $^{12}$C nucleus compared with the symmetric rotational model, namely, it has a smaller, prolate, quadrupole deformation as the equilibrium shape of the ground state. We have tried to find a possibility of getting a negative quadrupole deformation by changing the $\gamma_0$ parameter. We could obtain as good a fit as the result obtained by using the parameters explained previously to the level structure data with a value of $\gamma_0 = 2.82$, which gives a negative quadrupole deformation in our model through the factor $\beta_2 \cos(\gamma_0)$. We could also get a good fit to the elastic and inelastic scattering to the first excited $2^+$ state with this $\gamma_0$ value as the one with the previous parameter set. However, the fit to the other states became drastically worse, an example of such is shown in Fig. 7 as the broken curves for the $3^-$ level. In our model, the sign of the quadrupole deformation has a big impact on the inelastic scattering to, e.g., the octupole state, through the coupling term $\beta_2\beta_3$ which is absent in all of the previous analyses[4, 5]. Our model, which includes all of these cross-band coupling terms explicitely, strongly suggests that the quadrupole deformation must be positive. We understand that the positive quadrupole deformation is in contracdition to the results of microscopic RGM calculation[3]. On the other hand, the prolate deformation obtained in our analysis is in good accord with the concept of the "linear-chain structure" of 3 $\alpha$ particles proposed for the excited states of $^{12}$C long ago by Morinaga[29]. Possibility of such a shape is also mentioned by Uegaki et al.[2] Our model (and all of the previous analyses[4, 5]) does not allow $^{12}$C nucleus to change from the oblate to prolate deformation as the

of coupling probabilities of $\gamma$-transition from and to different levels are enhanced differently coupling with the rigid rotator model.

We compared the $B(E2)$ transition probability with the experimental data. Our model predicts 0.00418 $e^2b^2$ while the experimental value is $0.0041e^2b^2$[28]. Considering the fact that no parameter was adjusted to calculate this quantity, the agreement can be marked to be fantstic.

## 5. Discussion

According to the microscopic 3$\alpha$ cluster model[2, 3], the $0_1^+$, $2_1^+$ (4.44MeV) and $4_1^+$ (14.08MeV) are classified to form a ground state rotational band with a compact 3$\alpha$-cluster configurations around an equilateral triangle. Although the present model does not take account of such $\alpha$-cluster structure, the classification into a rotational band is also achieved in our model. The energy of the $4_1^+$ state is slightly less than the one expected from the rigid rotor model if the moment of inertia is calculated according to the energy of the $2_1^+$ state. The soft-rotator model accounts for such a stretching effect, as shown in Fig. 1. Firthermore, the $\alpha$ cluster model suggest a strong K-mixing in the $2_2^+$ and $3^+$ states, which is in good agreement with the present result because of the large $\gamma_0$ value.

In previous works[4, 5], the symmetric rotational model was employed to analyze the neutron scattering data, and $^{12}$C was assumed to have a large oblate deformation ($\beta_2 \approx$ -0.6), which is in good accord with the microscopic $\alpha$ cluster model[3]. On the other hand, there is no symmetry axis in the present tri-axial model. Indeed, the non-axiality parameter has a large value ($\gamma_0 = 0.3210$) compared with the case for actinide, so the axial symmetry is broken to a large extent in $^{12}$C. Therefore, the present model gives a different picture of $^{12}$C nucleus compared with the symmetric rotational model, namely, it has a smaller, prolate, quadrupole deformation as the equilibrium shape of the ground state. We have tried to find a possibility of getting a negative quadrupole deformation by changing the $\gamma_0$ parameter. We could obtain as good a fit as the result obtained by using the parameters explained previously to the level structure data with a value of $\gamma_0 = 2.82$, which gives a negative quadrupole deformation in our model through the factor $\beta_2 \cos(\gamma_0)$. We could also get a good fit to the elastic and inelastic scattering to the first excited $2^+$ state with this $\gamma_0$ value as the one with the previous parameter set. However, the fit to the other states became drastically worse, an example of such is shown in Fig. 7 as the broken curves for the $3^-$ level. In our model, the sign of the quadrupole deformation has a big impact on the inelastic scattering to, e.g., the octupole state, through the coupling term $\beta_2\beta_3$ which is absent in all of the previous analyses[4, 5]. Our model, which includes all of these cross-band coupling terms explicitely, strongly suggests that the quadrupole deformation must be positive. We understand that the positive quadrupole deformation is in contracdition to the results of microscopic RGM calculation[3]. On the other hand, the prolate deformation obtained in our analysis is in good accord with the concept of the "linear-chain structure" of 3 $\alpha$ particles proposed for the excited states of $^{12}$C long ago by Morinaga[29]. Possibility of such a shape is also mentioned by Uegaki et al.[2] Our model (and all of the previous analyses[4, 5]) does not allow $^{12}$C nucleus to change from the oblate to prolate deformation as the

excitation energy changes. Therefore, the prolate deformation we obtained presently may indicate that $^{12}$C nucleus is represented, when averaged over many states, by a prolate shape inspite of the proposed compact equilateral triangular shape for the ground state. Furthermore, an analysis of the spin-flip probability in proton inelastic scttering, which is sensitive to the sign of the quadrupole deformation, is not necessariry consistent with the oblate deformation (see Fig. 2 of Ref. [30]). Anyway, we must conclude that a small prolate quadruple deformation is required as the equilibrium shape of the ground state of $^{12}$C in the context of the soft-rotator model to describe the level structure, B(E2) and neutron interaction data consistently in a unified framwork.

We discuss in detail our calculations of scattering data for $4^+$ (14.08 MeV) level. This level was included in our scheme, additional coupling associated with this level is shown on Fig. 2 by thin lines. The result of calculations is in Fig. 8. They are by 25% higher than those calculations of [4] and describe experimental data very well. Now we are coming to the main point of our discussion - the advantage of our model.

We can compare the absolute value of $\beta_2 = 0.6$ [4] with our $\langle 0^+|\beta_2|2^+\rangle = 0.57$. The results almost coincide for the $2^+$ (4.44 MeV) state, but if we compare $\beta_2^2$ and $\langle 0^+|\beta_2^2|4^+\rangle$ that mainly determine one step excitation of the $4^+$ state, our value is approximately 30% higher and $\langle 0^+|\beta_2|2^+\rangle\langle 2^+|\beta_2|4^+\rangle$ determining two step excitation of the $4^+$ state is $\sim$10 % higher than those given in the rigid rotator model, that leads to 25% higher prediction of $4^+$ scattering data compared with the rigid rotator model. Our $\langle 0^+|\beta_2^2|0_2^+\rangle$ value determining one step excitation of the $0_2^+$ (7.65 MeV) level is 20 % lower than $\beta_2^2$ [4] and $\langle 0^+|\beta_2|2^+\rangle\langle 2^+|\beta_2|0_2^+\rangle$ determining two step excitation strength is 2.5 times lower. Accounting for this difference result in a fine description of angular distributions of neutrons scattered by the $0_2^+$ level. Thus the present model predicts a redistribution of coupling strength better compared with the model adopted in Ref. [4]. This allowed us to describe experimental angular distributions for the $0_2^+$ level without including $2_2^+$ level, which is not experimentally identified, in the coupling scheme as needed in calculations without the coupling strength redistribution[4]. It is the result of the stretching of a soft rotating $^{12}$C nucleus incorporated in the present model. Furthremore, we did not need to adopt the channel-energy dependent coupling potential, which was required in the rigid rotator model in Ref. [4], to reproduce the $2^+$ and $4^+$ member of the ground state rotational band.

It is also possible to compare the value $\langle 0^+|\beta_3|3^-\rangle = 0.404$ with the rigid $\beta_3$= 0.51 from Olsson et al.[5] We see that they coincide with reasonable accuracy. It is easy to account for the smaller value obtained in the present work. In the present model, such coupling terms as $\langle 0^+|\beta_2\beta_3|3^-\rangle$ and $\langle 0^+|\beta_4\beta_3|3^-\rangle$ are included, which are absent in the analysis by Olsson et al.[5] Furtheremore, we did not need to include the reaction mechanisms such as diffuseness oscillation and potential depth oscillation which were used by Meigooni et al.[4], to describe the cross sections leading to the vibrational bands.

The total, elastic scattering and inelastic neutron scattering cross sections to various collective bands in $^{12}$C were described in a unified manner in terms of the soft-rotator model, which can describe the collective level structure very well, without introducing any other reaction mechanisms which require additional parameters and hence make the discussion rather ambiguous.

# 6. Concluding remarks

The soft-rotator model was applied to analyse the collective nuclear level structure of $^{12}$C. Taking account of the non-axial quadrupole, octupole and hexadecapole deformations, and quadrupole and octupole vibrations, the level structure of $^{12}$C was reproduced successfully by this model. The intrinsic wave function thus obtained was then used to calculate the coupling potentials to be used in the coupled-channels theory, which yielded also satisfactory results when applied to neutron scattering data. The "equilibrium" quadrupole deformation was found to be 0.164, which then gives an "effective" deformation of 0.57 when averaged by the $\beta_2$ oscillation function. This fact shows how the $^{12}$C is soft in such a degree-of-freedom, a feature that is not incorporated in the rigid-rotator model frequently employed. The B(E2) value was also reproduced quite well by the model without any parameter adjustment. Therefore, we can conclude that the soft-rotator model gives a unified description of nuclear structure and neutron scattering data not only for the actinide nuclei (where this theory has been intensively applied) but also for such a light mass region as the 1p shell nuclei. Continuation of such analyses performed in this work for other nuclei will be of great importance for the understanding the collective nature of nuclei, and also from the applications point of view.

The sign of the quadrupole deformation was definitely required to be positive in our model which takes account of all the cross-band coupling terms explicitely; a feauture absent in previous works. The interpretation of this result may leave a room for a controversy. We think that it is related with the proposed linear-chain structure of 3 $\alpha$ particles for excited states, or at least a kind of "effective" shape when averaged over many states. Such a new interpretation may, we hope, lead to a better understanding of the nature of this and other nuclei in this mass region, where only little is known to date.

# Acknowledgements

The authors are grateful to Dr. Mark B. Chadwick of LANL for stimulating discussions. One of the authors, E. Soukhovitski, is grateful to JAERI for offering an opportunity to stay at JAERI via foreign scientist invitation program which made this work possible.

# 6. Concluding remarks

The soft-rotator model was applied to analyse the collective nuclear level structure of $^{12}$C. Taking account of the non-axial quadrupole, octupole and hexadecapole deformations, and quadrupole and octupole vibrations, the level structure of $^{12}$C was reproduced successfully by this model. The intrinsic wave function thus obtained was then used to calculate the coupling potentials to be used in the coupled-channels theory, which yielded also satisfactory results when applied to neutron scattering data. The "equilibrium" quadrupole deformation was found to be 0.164, which then gives an "effective" deformation of 0.57 when averaged by the $\beta_2$ oscillation function. This fact shows how the $^{12}$C is soft in such a degree-of-freedom, a feature that is not incorporated in the rigid-rotator model frequently employed. The B(E2) value was also reproduced quite well by the model without any parameter adjustment. Therefore, we can conclude that the soft-rotator model gives a unified description of nuclear structure and neutron scattering data not only for the actinide nuclei (where this theory has been intensively applied) but also for such a light mass region as the 1p shell nuclei. Continuation of such analyses performed in this work for other nuclei will be of great importance for the understanding the collective nature of nuclei, and also from the applications point of view.

The sign of the quadrupole deformation was definitely required to be positive in our model which takes account of all the cross-band coupling terms explicitely; a feauture absent in previous works. The interpretation of this result may leave a room for a controversy. We think that it is related with the proposed linear-chain structure of 3 $\alpha$ particles for excited states, or at least a kind of "effective" shape when averaged over many states. Such a new interpretation may, we hope, lead to a better understanding of the nature of this and other nuclei in this mass region, where only little is known to date.

# Acknowledgements

The authors are grateful to Dr. Mark B. Chadwick of LANL for stimulating discussions. One of the authors, E. Soukhovitski, is grateful to JAERI for offering an opportunity to stay at JAERI via foreign scientist invitation program which made this work possible.

# References


[1] Cohen S., Kurath D.: Nucl. Phys. **73**, 1(1965).

[2] Uegaki E., Okabe S., Abe Y., Tanaka H.: Prog. Theor. Phys. **57**, 1262(1977).

[3] Kamimura M.: Nucl. Phys. **A351**, 456(1981).

[4] Meigooni A., Finlay R.W., Petler J.S., Delaroche J.P.: Nucl. Phys. **A445** 304 (1985)

[5] Olsson N., Trostell B., Ramström E.: Nucl. Phys. **A496** 505(1989)

[6] Winfield J.S., Austin Sam M., DeVito R.P., Berg U.E.P., Chen Ziping, Sterrenburg W.: Phys. Rev. **C33**, 1(1986).

[7] Niizeki T., Orihara H., Ishii K., Maeda K., Kabasawa M., Takahashi Y., K. Miura: Nucl. Instr. Meth. **A287**, 455(1990).

[8] Davydov A.S., Chaban A.A.: Nucl. Phys. **20**, 499(1960).

[9] Porodzinski Y.V.i̇, Sukhovitskiĭ E.S.: Sov. J. Nucl. Phys. **53**, 41(1991).

[10] Porodzinskiĭ Y.V., Sukhovitskiĭ E.S.: Sov. J. Nucl. Phys. **54**, 570(1991).

[11] Porodzinskiĭ Y.V., Sukhovitskiĭ E.S.: Sov. J. Nucl. Phys. **55**, 1315(1992).

[12] Porodzinskiĭ Y.V., Sukhovitskiĭ E.S.: Phys. At. Nucl. **56**, 1336(1993).

[13] Porodzinskiĭ Y.V., Sukhovitskiĭ E.S.: Phys. At. Nucl. **59**, 228(1996).

[14] Bohr A., Mottelson B.R.: "Nuclear Structure, Vol. II, Nuclear Deformations", p.195, W.A. Benjamin Inc. (1975).

[15] Davydov A.S.: "Vozbuzhdennye sostoyaniya atomnykh yader (Excited States of Atomic Nuclei)", Moscow: Atomizdat (1969)

[16] Lipas P.O., Davidson J.P.: Nucl. Phys. **26**, 80(1961)

[17] Rohozinski S.G., Sobiczewski A.: Acta. Phys. Polon. **B12**, 1001(1981)

[18] Strutinsky I.M.: At. Energ. **4**, 150(1956)

[19] Flugge S.: "Practical Quantum Mechanics", Springer-Verlag, Berlin-Heidelberg-New York, 1971

[20] Dzyublik A.Ya., Denisov V.Yu.: Yad. Fiz. **56**, 30(1993)

[21] Eisenberg J.M., Greiner W.: "Nuclear Models", North-Holland (1970).

[22] Davydov A.S., Filippov G.F.: Nucl. Phys. **8**, 237(1958).

[23] Abramowitz M., Stegun I.A.: "Handbook of Mathematical Functions", Dover Publications, New York(1965).

[24] Tamura T.: Rev. Mod. Phys. 37, 679(1965).

[25] Yamanouti Y., Sugimoto M., Chiba S., Mizumoto M., Hasegawa K. , Watanabe Y.: Proc. Int. Conf. Sci. and Tech., 13-17 May, 1991, Juelich, Germany, p.717(1992).

[26] Ajzenberg-Seleve F.: Nucl. Phys. **A506** (1990)

[27] Finlay R.W., Abfaltere W.P., Fink G., Montei E., Adami T., Lisowski P.W., Morgan G.L., Haight R.C.: Phys. Rev. **C47**, 237(1993j).

[28] Raman, S., Malarkey C.H., Milner W.T., Nestor Jr. C.W., Stelson P.H.: At. Data and Nucl. Data Tables **36**, 1(1987).

[29] Morinaga H.: Phys. Rev. **101**, 254(1956); Phys. Letters **21**, 98(1966).

[30] De Leo R., D'Erasmo G., Fiore E.M., Guarino G., Pantaleo A., Micheletti S., Pignanelli M., Serafini L.: Phys. Rev. **C25**, 107(1982).

Table 1: The nuclear Hamiltonian parameters which are adjusted to reproduce the experimental level scheme

| | | |
|---|---|---|
| $\hbar\omega_0 = 4.2825$ | | |
| $\mu_{\beta_{20}} = 2.7943$ | $\mu_{\gamma_0} = 0.1303$ | $\gamma_0 = 0.3210$ |
| $a_{32} = 0.2213$ | $\gamma_4 = 0.00021$ | $\delta_4 = 0.5205$ |
| $a_{42} = 0.1469$ | $\mu_\epsilon = 0.9083$ | |
| $\eta = 0.02101$ | $\delta_n = 1.7221$ | |

Table 2: Experimental scattering data involved in CC optical analysis

| Reference | Interaction Energy (MeV) | Spin, parity, energy of the excited level | | | | |
|---|---|---|---|---|---|---|
| | | $0^+(0.0)$ | $2^+(4.44)$ | $0^+(7.65)$ | $3^-(9.64)$ | $4^+(14.08)$ |
| Olsson et al.[5] | 20.9 | ○ | | ○ | ○ | |
| | 22.0 | ○ | ○ | ○ | ○ | |
| Meigooni et al.[4] | 20.8 | ○ | | ○ | ○ | |
| | 22.0 | ○ | ○ | ○ | ○ | |
| | 24.0 | ○ | ○ | ○ | ○ | ● |
| | 26.0 | ○ | ○ | ○ | ○ | |
| Yamanouti et al[25] | 28.2 | ○ | ○ | | ○ | |
| Niizeki et al.[7] | 35.0 | ● | | | | |
| Winfield et al.[6] | 40.3 | ○ | | | | |

○- data used for potential parameter adjustment

●- data used for comparison only

Table 3: The optical potential parameters allowing the best fit of experimental data

$$V_R = 53.11 - 0.436E$$

$$W_D = \begin{cases} 7.350 - 0.145E & E \leq 23 \\ 4.015 + 0.0043(E-23) & E > 23 \end{cases}$$

$$W_V = \begin{cases} 3.743 - 0.021E & E \leq 23 \\ 3.260 + 0.057(E-23) & E > 23 \end{cases}$$

$$V_{so} = 6.65$$

$r_R = 1.1935$ $\quad a_R = 0.552 + 0.00318E$

$$r_D = 1.1321 \quad a_D = \begin{cases} 0.336 + 0.0034E & E \leq 23 \\ 0.4142 & E > 23 \end{cases}$$

$r_V = 1.1971$ $\quad a_V = 0.311 + 0.00255E$

$r_{so} = 1.2001$ $\quad a_{so} = 0.559$

$\beta_{20} = 0.164$ $\quad \beta_{30} = \beta_{20}\epsilon_0 = 0.0433$ $\quad \beta_4 = 0.116$

Strength and incident energy $E$ in MeV; radii and diffusenesses in fm.

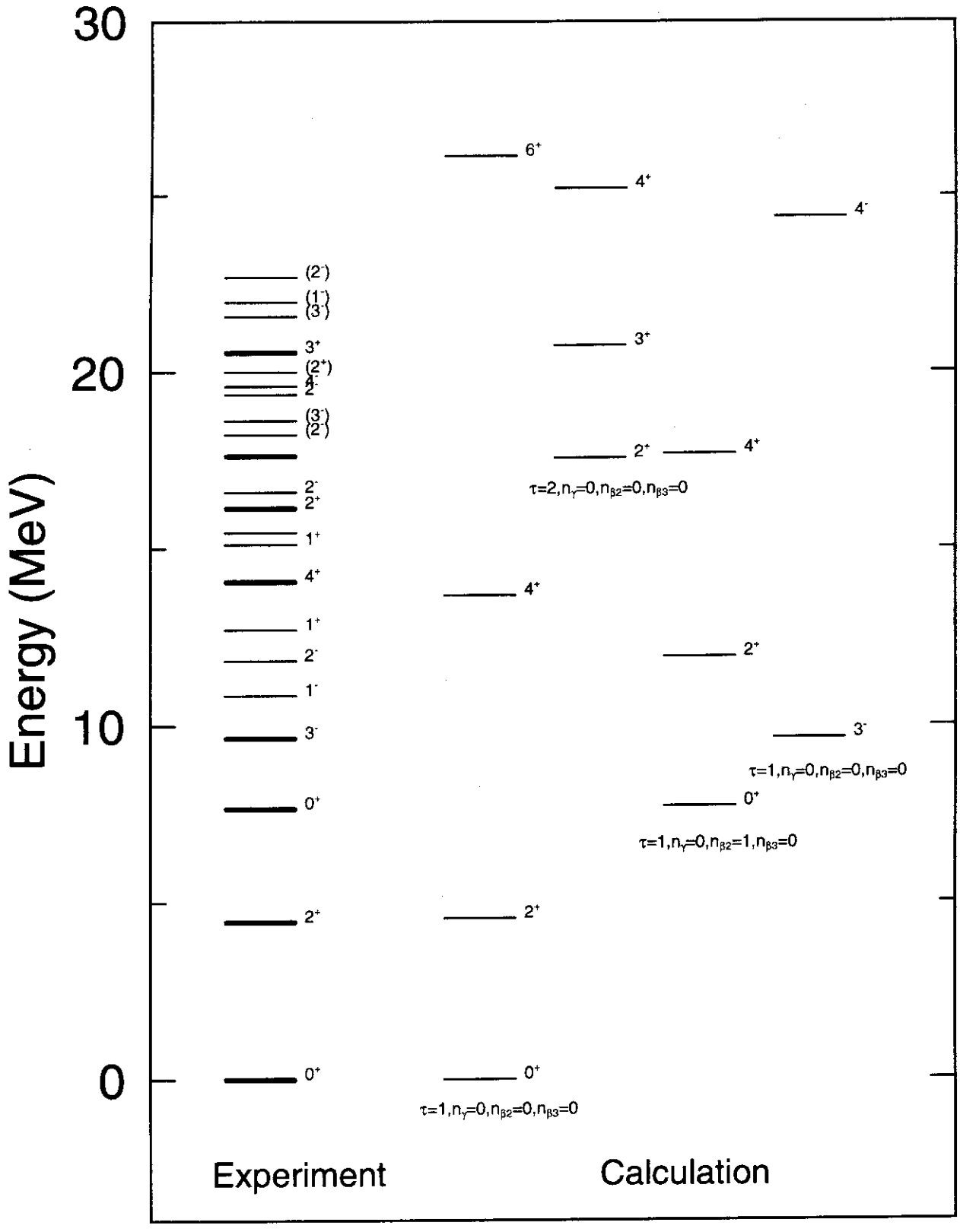


Fig. 1: Comparison of experimental and calculated level schemes. Thick lines show experimental levels described by the soft-rotator model.

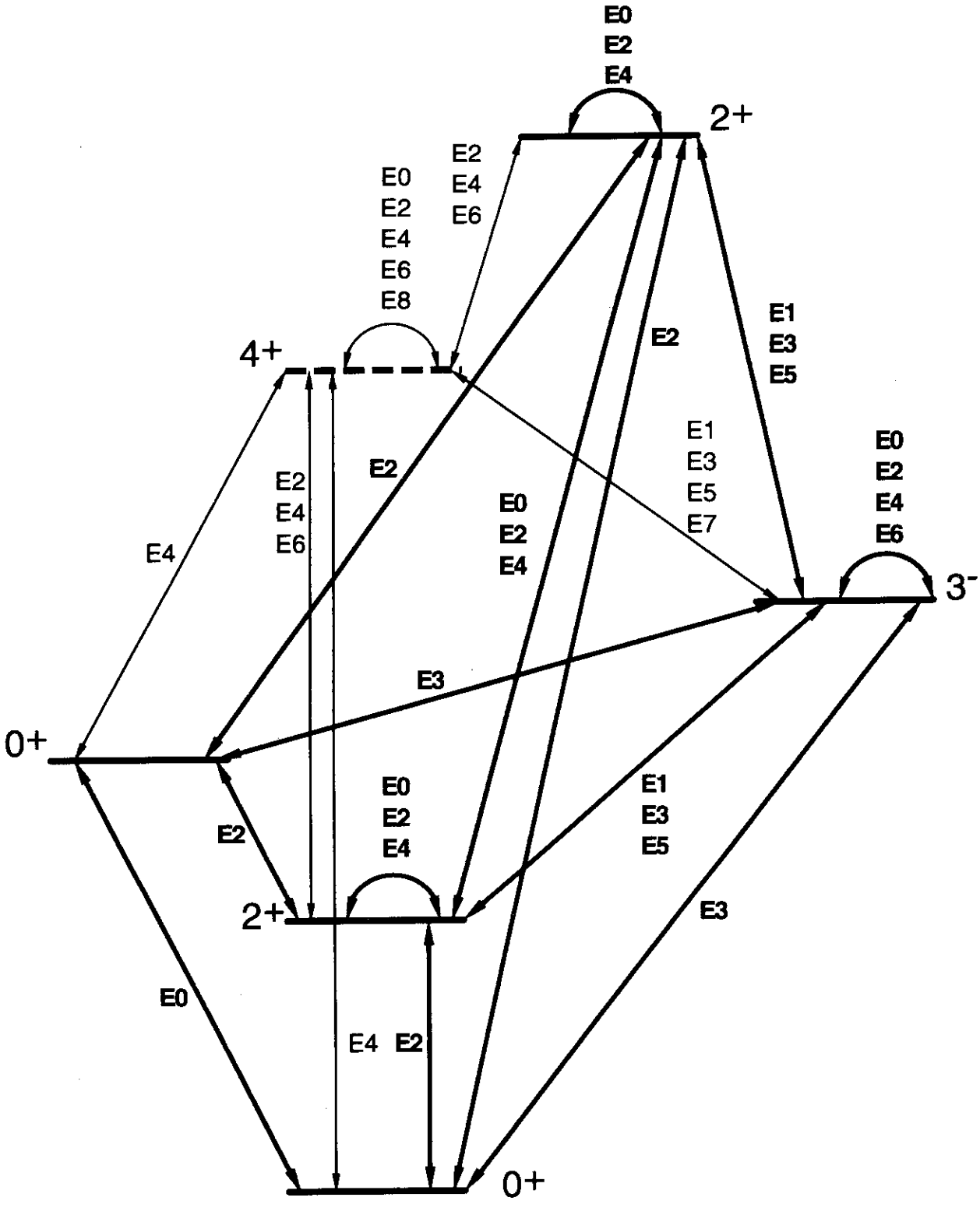


Fig. 2: Coupling scheme employed in the present calculation. Thick arrows show coupling used in the parameter search procedure. Thin arrows additional coupling arising when $4^+$ (14.08 MeV) level is added used.

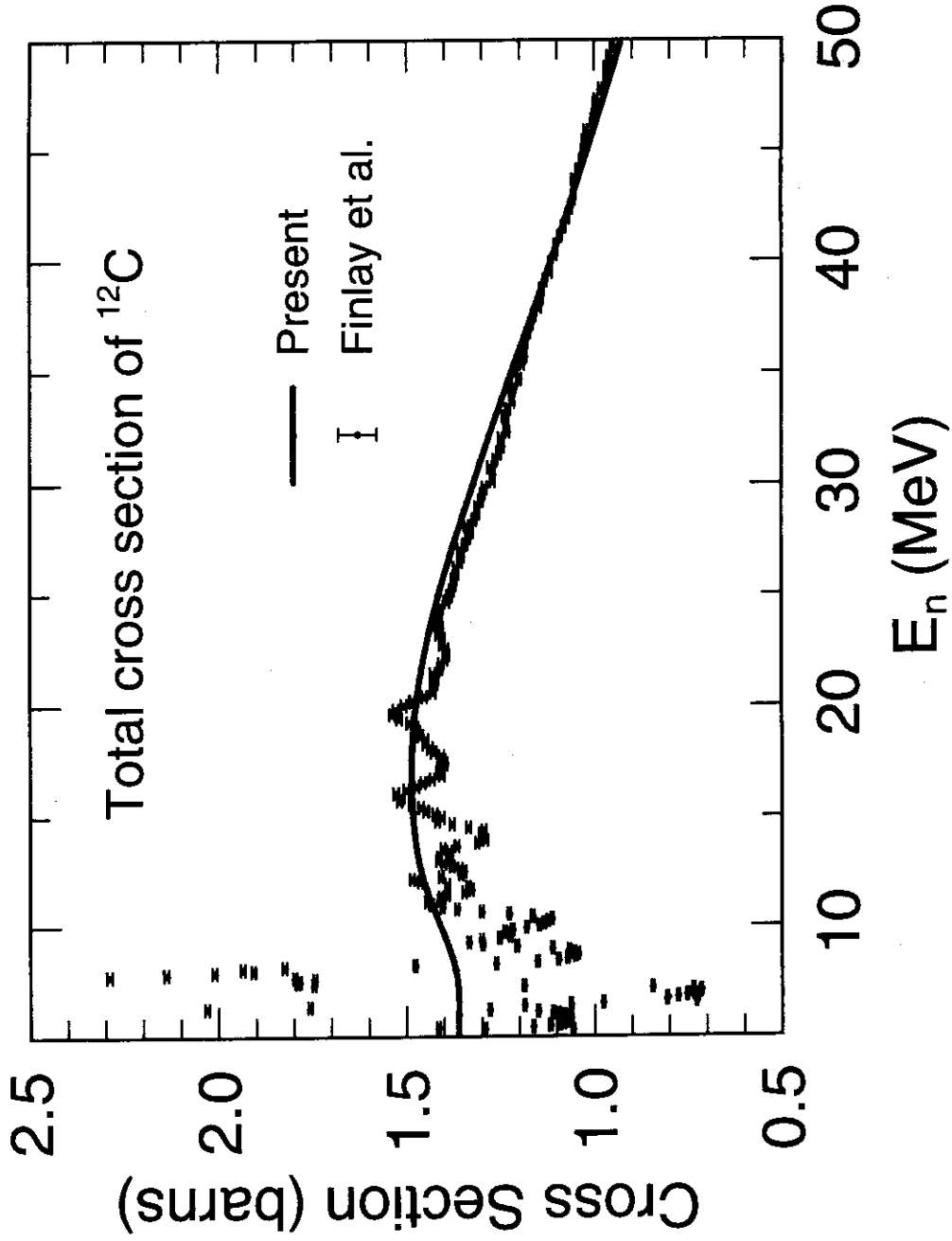


Fig. 3: Comparison of experimental and calculated $^{12}$C total cross section.

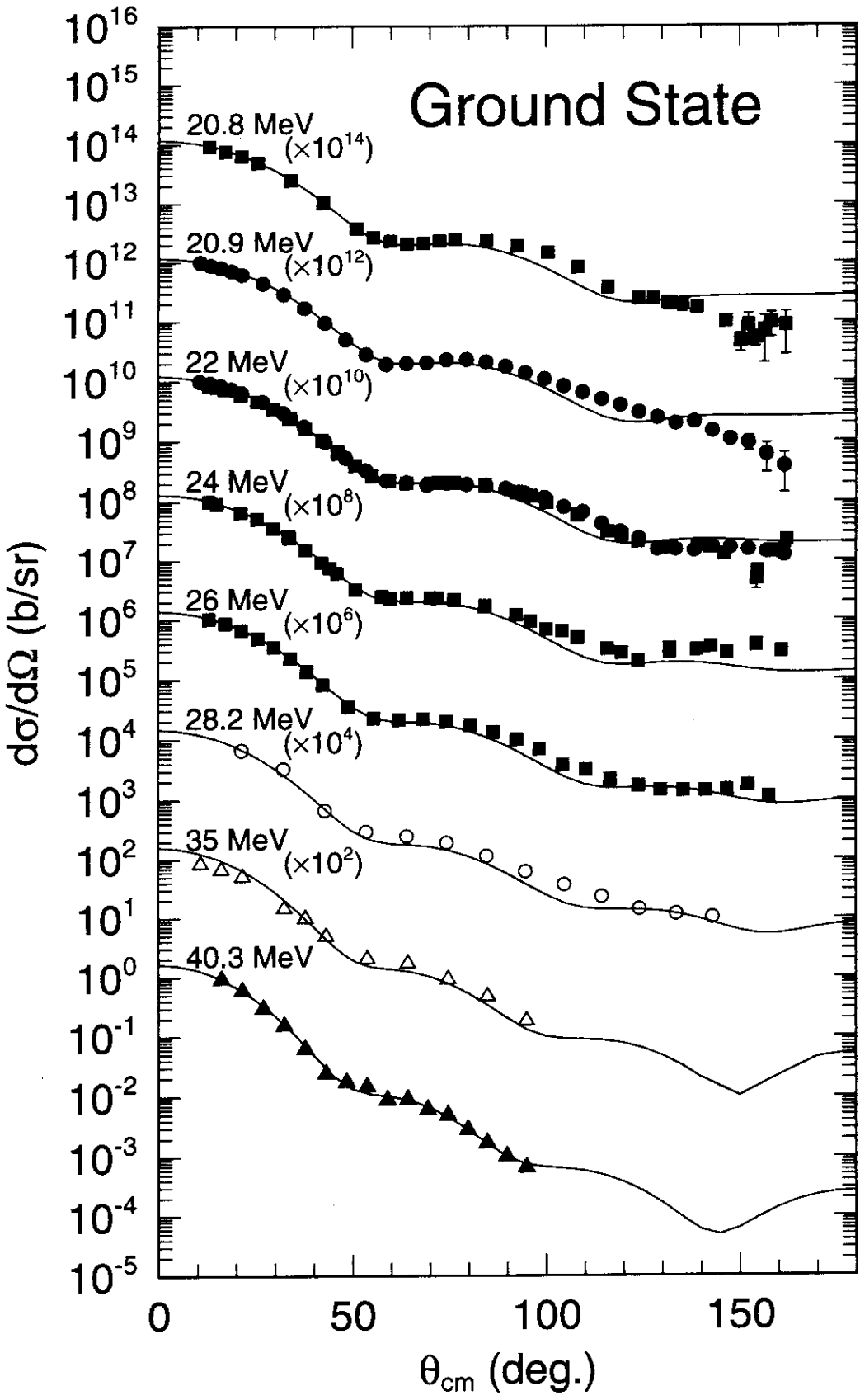


Fig. 4: Comparison of experimental and calculated angular distributions for elastically scattered neutron. Solid line : Present calculation, Closed circles : Olsson et al.,squares : Meigooni et al., open circle : Yamanouti et al., open triangle at 35 MeV : Niizeki et al., and triangle : DeVito

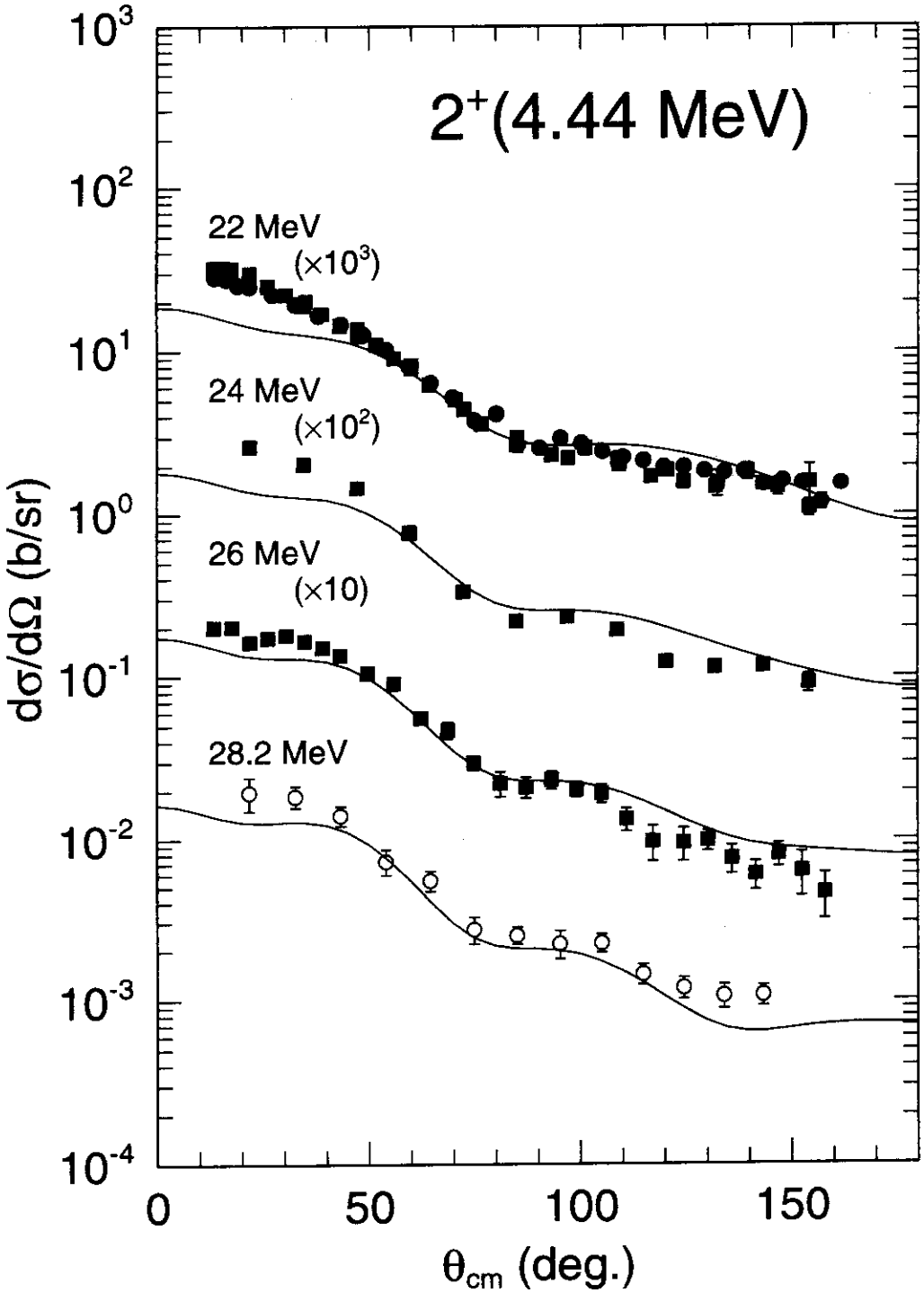


Fig. 5: Comparison of experimental and calculated angular distributions for neutrons scattered by $2^+$ (4.44 MeV). Assignment of the experimental data are the same as Fig. 4 in this and subsequent figures.

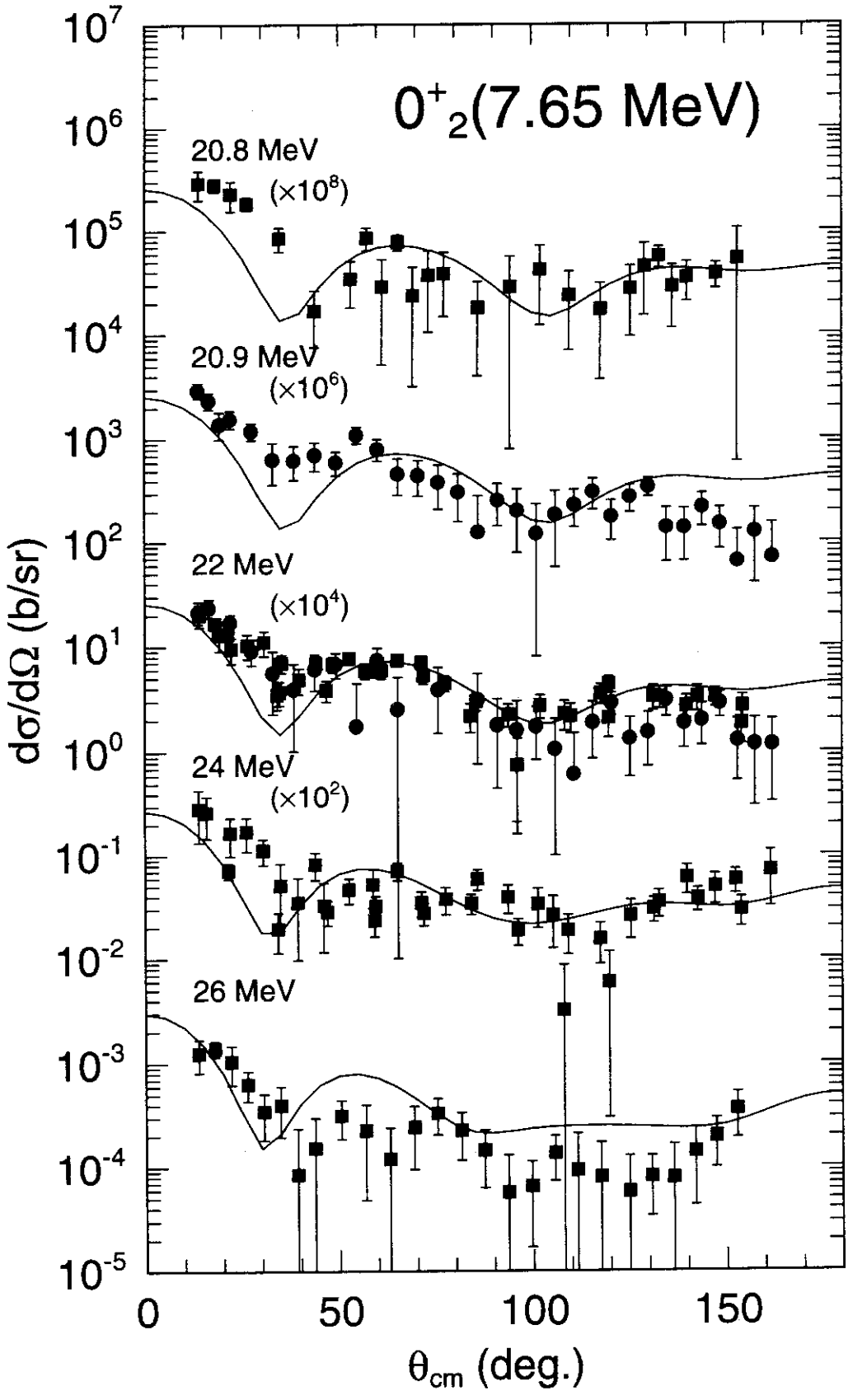


Fig. 6: Comparison of experimental and calculated angular distributions for neutrons scattered by $0^+_2$ (7.65 MeV).

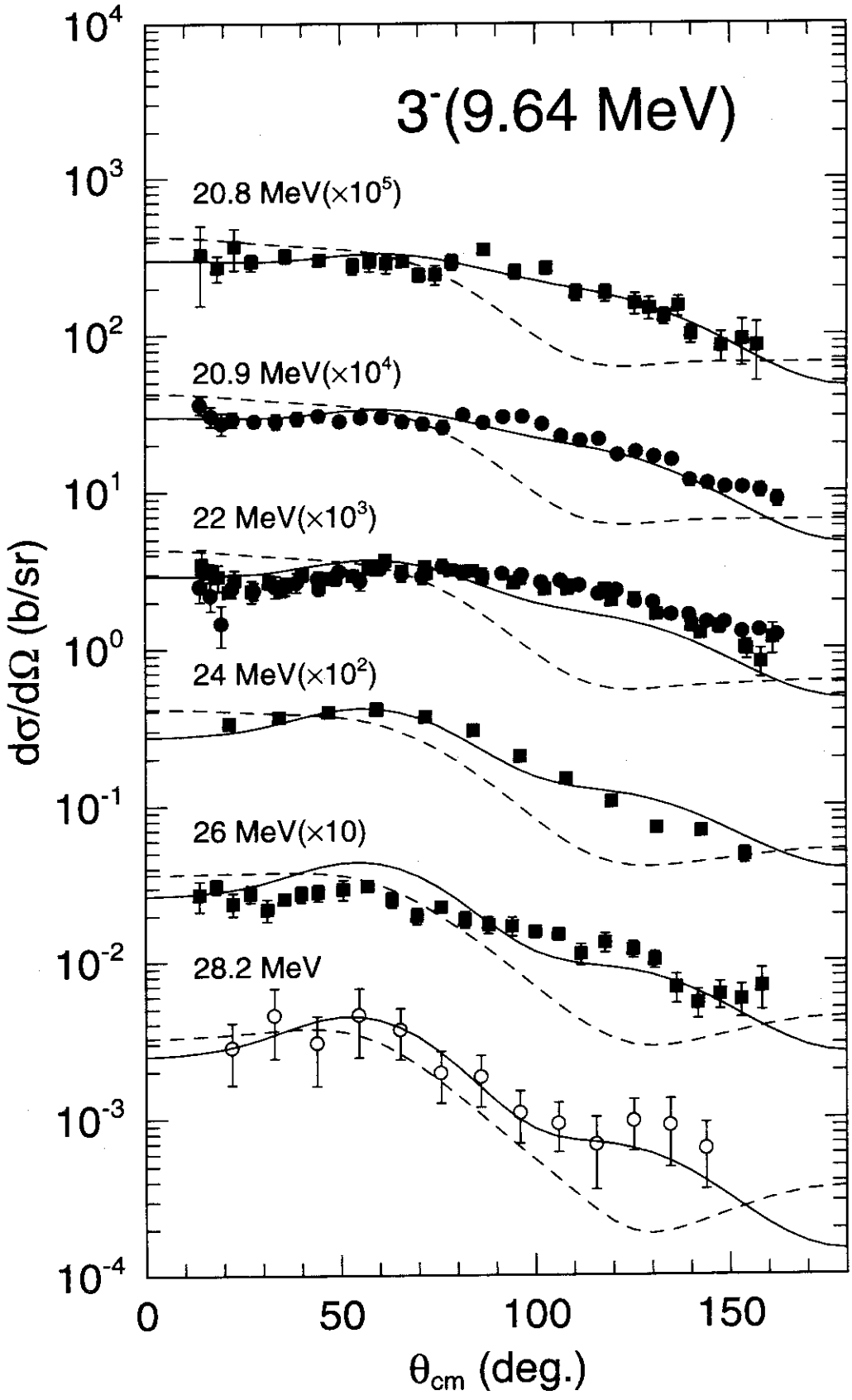


Fig. 7: Comparison of experimental and calculated angular distributions for neutrons scattered by $3^-$ (9.64 MeV). The solid lines show the calculated results with the parameters in Tables 1 and 3, while the broken curves correspond to a calculation with negative quadrupole deformation (see text for details).

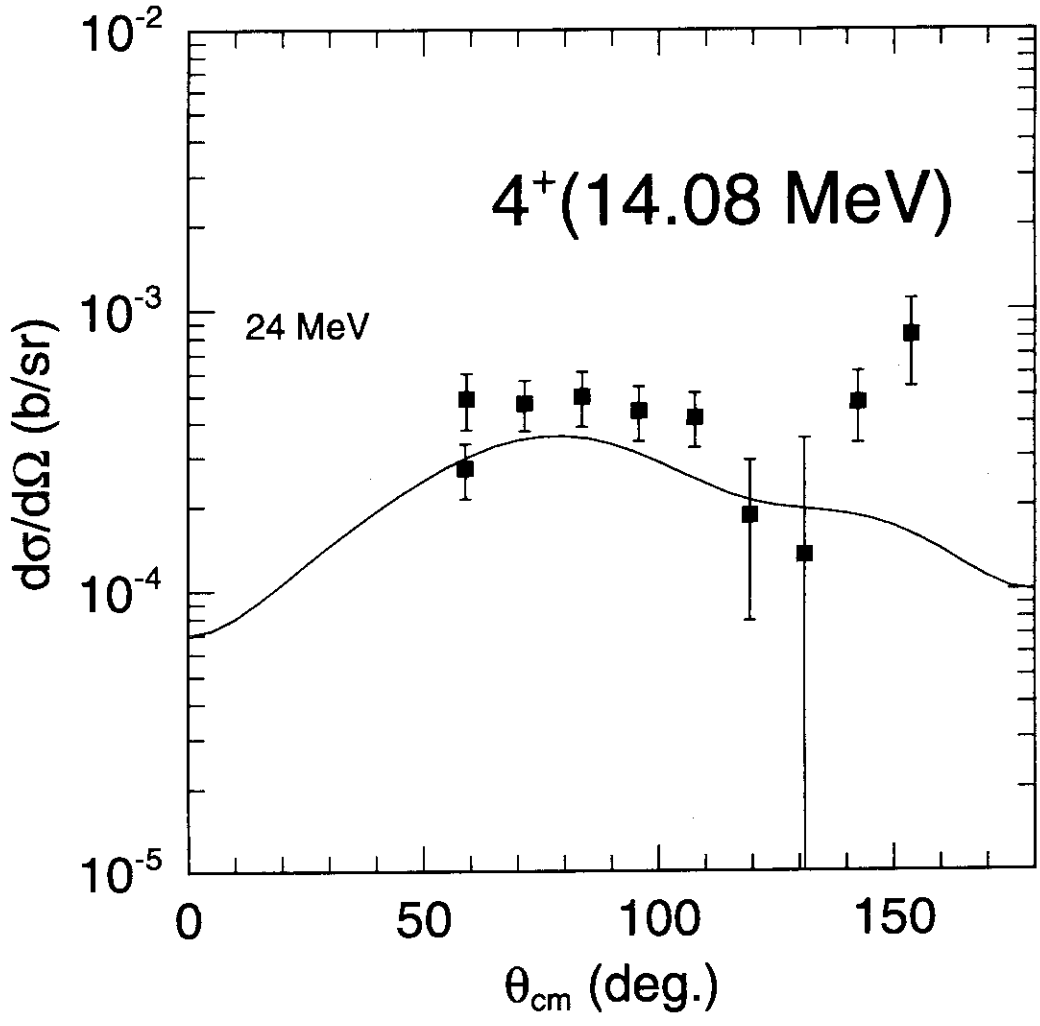


Fig. 8: Comparison of experimental and calculated angular distributions for neutrons scattered by $4^+$ (14.08 MeV).